

A new limit on the permanent electric dipole moment of ^{199}Hg .

M.V. Romalis, W.C. Griffith, and E.N. Fortson

Department of Physics, University of Washington, Seattle, Washington 98195

(Submitted Nov 21, 2000)

We present the first results of a new search for a permanent electric dipole moment of the ^{199}Hg atom using a UV laser. Our measurements give $d(^{199}\text{Hg}) = -(1.06 \pm 0.49 \pm 0.40) \times 10^{-28} e\text{cm}$. We interpret the result as an upper limit $|d(^{199}\text{Hg})| < 2.1 \times 10^{-28} e\text{cm}$ (95% C.L.), which sets new constraints on $\bar{\theta}_{\text{QCD}}$, chromo-EDMs of the quarks, and CP violation in Supersymmetric models.

PACS Numbers: 11.30.Er,32.10.Dk,32.80.Bx

In order for an elementary particle, atom, or molecule to have a permanent electric dipole moment (EDM) time reversal symmetry must be violated. By the CPT theorem it also implies a violation of CP symmetry. A finite EDM would give an unambiguous signal of CP violation beyond the Standard Model (SM), since EDMs caused by CP violation in the SM are negligible. Most extensions of the SM, such as Supersymmetry, naturally produce EDMs that are comparable to or larger than present experimental limits [1]. Additional sources of CP violation are motivated by theories of baryogenesis [2].

Experimental searches for EDMs can be divided into three categories: search for the neutron EDM [3], search for the electron EDM utilizing paramagnetic atoms or molecules, the most sensitive of which is done with Tl atoms [4], and search for an EDM of diamagnetic atoms, the most sensitive of which is done with ^{199}Hg [5]. The limits set by the most sensitive experiments in each category are comparable, and they constrain different combinations of CP-violating effects [1].

Here we present the first results of a new search for a permanent EDM of the ^{199}Hg atom. Using a substantially different experimental technique we reduce the limit on the ^{199}Hg EDM by a factor of 4. To detect the EDM we measure the Zeeman precession frequency of ^{199}Hg nuclear spins ($I = 1/2$) in parallel electric and magnetic fields. The measurements are simultaneously performed in two cells with oppositely directed electric fields to reduce the frequency noise due to magnetic field fluctuations. A difference between the Zeeman frequencies in the two cells correlated with reversals of the direction of the electric field E is proportional to the EDM d ,

$$\hbar(\omega_1 - \omega_2) = 4dE.$$

An overall schematic of the apparatus is shown in Figure 1. Isotopically enriched ^{199}Hg vapor (92% ^{199}Hg) was contained in quartz cells with a conductive SnO coating chemically deposited on the inside surfaces to apply an electric field. The distance between the electric field plates was 11 mm. A small excess of ^{199}Hg deposited in the stem of the cells maintained the number density of ^{199}Hg atoms close to the room temperature vapor pres-

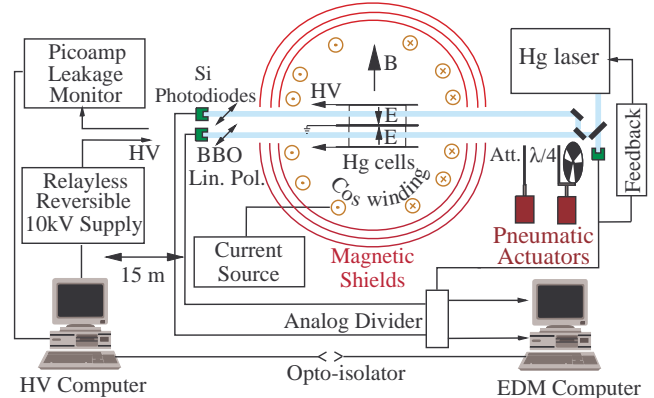


FIG. 1. Schematic of the apparatus used to search for a permanent EDM of ^{199}Hg atoms.

sure. The cells also contained 450 torr of N_2 gas and 50 torr of CO gas. The walls of the cells were coated with paraffin ($\text{C}_{32}\text{H}_{66}$) to increase the spin relaxation time. The paraffin was remelted after the cells were sealed to obtain a thin transparent coating. After such remelting the ^{199}Hg spin coherence time was typically about 300-500 sec. However, after a week of continuous UV exposure the lifetime would drop to below 100 sec. We believe this was due to damage of the paraffin coating caused by collisions with Hg atoms in the metastable 6^3P_0 state, to which they are quenched by N_2 gas. CO gas is effective in quenching ^{199}Hg atoms to the ground state. The spin coherence time could be restored by remelting the paraffin coating. The cells were placed in a sealed vessel made from carbon-filled conductive polyethylene and filled with SF_6 gas. It was located inside a three layer magnetic shield with a shielding factor of 5×10^4 . A magnetic field of 15 mG was maintained inside the shields by an ultra-low noise current source [7]. On a time scale of 100 sec the field was stable to 25 ppb.

Optical pumping and detection was done using a laser operating at the $253.7 \text{ nm } 6^1S_0 \rightarrow 6^3P_1$ transition of Hg. To generate this wavelength we quadrupled the output of a semiconductor MOPA (Master Oscillator Power Amplifier) laser operating at 1015 nm [6]. We obtained up to 6 mW of UV light. A feedback system adjusted the current of the power amplifier to keep the light intensity

constant. The intensity noise was $10^{-4}/\sqrt{\text{Hz}}$ at 10 Hz. The output of the laser was split into two beams directed perpendicular to the magnetic and electric fields. For optical pumping the light was circularly polarized and tuned to the center of the $F = 1/2$ hyperfine line of the $6^1S_0 \rightarrow 6^3P_1$ transition. It was chopped at the Larmor frequency of ^{199}Hg spins with a duty cycle of 30%, building-up the polarization in the rotating frame. To measure the frequency of spin precession the polarization of the light was switched to linear, the frequency detuned from resonance by 20 GHz, and the intensity attenuated to about $7 \mu\text{W}$. Precessing ^{199}Hg spin polarization produced an optical rotation of about 60 mrad giving a 50% modulation of the intensity transmitted through BBO Glan-laser polarizers.

A single measurement typically consisted of a 30 sec pump phase and 100 sec probe phase. During the pump phase the direction of the electric field was reversed. The high voltage (HV) applied to each cell was typically alternated between 10 kV and -10 kV. A solid-state relayless HV power supply was used to reduce the magnetic fields correlated with HV. All HV-related equipment was located 15 m away from the magnetic shields. We also occasionally skipped a HV reversal to guard against correlations with periodic fluctuations. The leakage currents flowing on the walls of the cells and the vessel were measured using current monitors with noise less than 0.1 pA. The vessel was designed to provide a symmetric current path for the charging and leakage currents, so the magnetic field created by the currents had only a small projection onto the main magnetic field. The charging currents, which were on the order of 1 nA, did not produce an observable EDM signal even when the electric field was reversed during the probe phase. We also continuously monitored 12 other signals, including three components of the magnetic field outside of the shields, the position of the laser beam transmitted through the cell, and several laser parameters.

A typical run lasted about one day and consisted of several hundred individual measurements. Each of the spin precession signals was digitally filtered using a band-pass FFT filter and fit to an exponentially-decaying sine wave to determine its frequency and other parameters. The scatter between successive frequency measurements was due to phase noise and magnetic field noise. We estimated the contribution from the phase noise by splitting the signal into short time intervals and fitting them individually. We verified that the whole detection system was working within 50% of fundamental shot-noise limitations. The correlation between the Zeeman frequency difference and the direction of the electric field was calculated by analyzing groups of 3 consecutive measurements and eliminating a linear frequency drift. In most runs the frequency noise due to magnetic field gradient fluctuations was comparable to the phase noise, typically increasing χ^2 for EDM correlations to about 2. The sta-

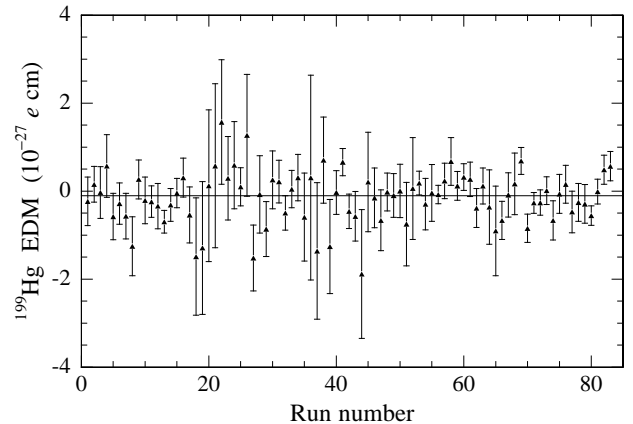


FIG. 2. ^{199}Hg EDM signal as a function of run number. The solid line shows the average of the data.

tistical error was increased by $\sqrt{\chi^2}$ to reflect actual data scatter in each run.

Frequent reversals and changes were done during the experiment to monitor for systematic effects. We periodically reversed the data acquisition channels for the two cells and the direction of the magnetic field, which should change the sign of the EDM signal. We also frequently changed the EDM cells and their orientation in the vessel. In addition, the paraffin in the cells was remelted and the outside surfaces cleaned each time the cells were changed, which would likely change the path of the leakage currents. Over the course of the experiment we used two different vessels and changed other components of the setup. Figure 2 shows the results of all EDM runs. The weighted average of all data gives $d(^{199}\text{Hg}) = -(1.06 \pm 0.49) \times 10^{-28} e \text{ cm}$. We do not observe any excess data scatter due to changes during the experiment and the χ^2 per degree of freedom is equal to 0.95. The statistical error corresponds to a frequency difference between the two cells of 0.4 nHz, a factor of 5 smaller than in the previous experiment [5].

We looked for systematic effects by changing the operating parameters of the experiment, exaggerating certain imperfections, and looking for correlations among different parameters. The leakage currents are a potentially serious source of systematic errors because they can produce magnetic fields that are correlated with the electric field and mimic an EDM signal. It should be noted that only leakage currents flowing in a helical path around the cell will contribute to first order. Figure 3 shows a scatter plot of the EDM signal vs. the leakage current in one of the cells. No statistically significant correlation was observed. The average cell leakage currents were about 0.6 pA. From the error on the correlation slope we can set a limit on the contribution of the leakage current to the EDM signal of $0.14 \times 10^{-28} e \text{ cm}$. We estimate the error more conservatively by calculating the magnetic field created by a leakage current making one complete loop

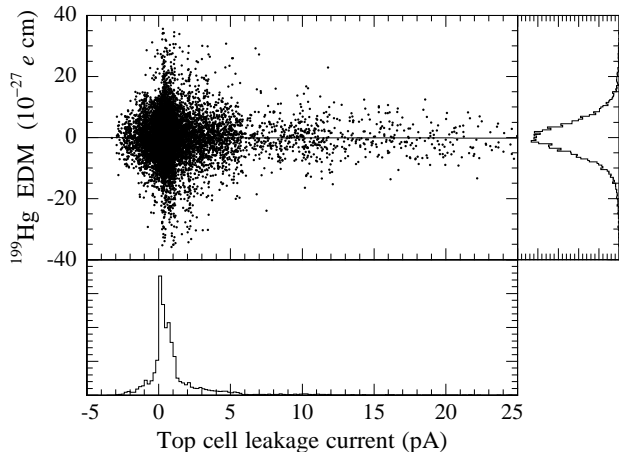


FIG. 3. Correlation between the leakage current and the EDM signal. Histograms of the leakage current and the EDM data are also shown. The solid line is a linear fit giving a correlation of $(-0.4 \pm 2.0) \times 10^{-29} e \text{ cm/pA}$.

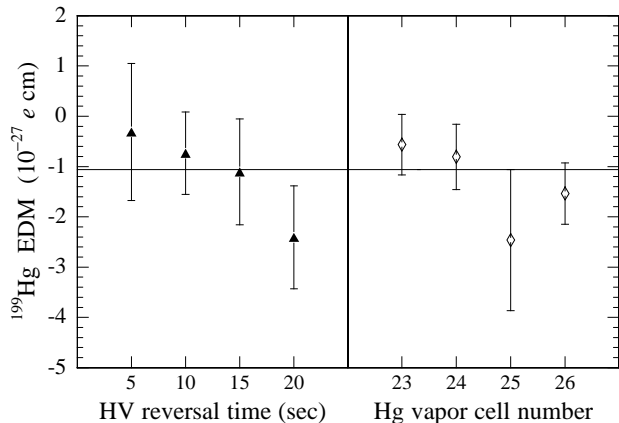


FIG. 4. The left panel shows the dependence of the EDM signal on the HV reversal time. The right panel shows the EDM signal obtained with each of the EDM cells. The solid line is an average of all data.

around the cell. This rather unlikely path would give an average EDM signal of $0.25 \times 10^{-28} e \text{ cm}$. A total of 4 vapor cells were used in the experiment in various pairs. The right panel of Figure 4 shows that the EDM data taken with each cell are consistent. Note that if a cell had a fixed helical path for the leakage current, it would produce the same EDM signal independent of the orientation of the cell. As can be seen in Figure 3, the leakage currents were sometimes negative. We believe this effect was due to changes in the mutual capacitance caused by redistribution of charges on HV insulators. If the HV was not reversed for a long time, the leakage currents became positive and approached a steady state value of about 0.1 pA.

We looked for correlations with the electric field of 30 other variables, such as monitored signals and fit-

ting parameters, and found no statistically significant correlations. Using random fluctuations of the variables we determined the cross-correlation between each of them and the EDM signal $\omega_1 - \omega_2$. In this way we set upper limits on false EDM signals coming from cross-correlations. All these limits are 10 to 100 times smaller than our statistical error. For positive direction of the magnetic field the average EDM signal was $d(B+) = -(1.78 \pm 0.70) \times 10^{-28} e \text{ cm}$ and for negative direction $d(B-) = -(0.36 \pm 0.69) \times 10^{-28} e \text{ cm}$. The two results are within 1.4σ of each other. A systematic effect that does not reverse with the magnetic field would show up in the difference but cancel in the average of the two results. To study possible frequency shifts due to magnetization of the magnetic shields caused by the charging currents, we varied the high voltage reversal time from 5 to 20 sec. The dependence of the EDM signal on the HV reversal time, shown in the left panel of Figure 4, is not statistically significant. We did not resolve any correlations of the individual Larmor frequencies ω_1 and ω_2 with the electric field outside of their error bars, which are a factor of 6 larger than the statistical error on $\omega_1 - \omega_2$.

We looked for effects proportional to E^2 in separate runs by applying the electric field to only one of the two cells and alternating the HV between 0 and ± 10 kV. The quadratic frequency shift was less than 2 nHz. We checked that the electric field in the cells was uniform and reversible with an accuracy of 1.5% [6], which limits the effect of reversal imperfections to less than $7 \times 10^{-30} e \text{ cm}$. Although the average velocity of the atoms in the cell is equal to zero, residual $v \times E$ effects [4] can exist if the surface relaxation on the walls is asymmetric. We looked for these effects by taking data with the magnetic field intentionally misaligned by 5° from the electric field. No effects were seen at the level of $1.5 \times 10^{-28} e \text{ cm}$, which can be used to constrain this effect to less than $0.3 \times 10^{-28} e \text{ cm}$ in a magnetic field aligned within 1° relative to the electric field. Among various frequency shifts caused by the probe light the most significant is due to the magnetic dipole and electric quadrupole transitions in an electric field [8]. This effect is odd in the E field and can mimic an EDM signal. It is suppressed to about $3 \times 10^{-30} e \text{ cm}$ because the laser beam is directed perpendicular to the magnetic field and detuned far from resonance.

In summary, no statistically significant systematic effects that mimic an EDM signal were observed, although in several cases our systematic studies were limited by statistics. We estimate the total systematic uncertainty to be $0.40 \times 10^{-28} e \text{ cm}$ by adding in quadrature the limits on systematic effects due to the leakage currents, the $v \times E$ effect, and other miscellaneous effects. Thus we obtain $d(^{199}\text{Hg}) = -(1.06 \pm 0.49 \pm 0.40) \times 10^{-28} e \text{ cm}$ and interpret the result as an upper limit on the ^{199}Hg EDM $|d(^{199}\text{Hg})| < 2.10 \times 10^{-28} e \text{ cm}$ (95% C.L.).

This limit can be used to place new constraints on

Parameter	Limit from ^{199}Hg	Best other limit	Th. Ref.
θ_{QCD}	1.5×10^{-10}	6×10^{-10} n [3]	[14,16]
\tilde{d}_d (cm)	7×10^{-27}	1.1×10^{-25} n [3]	[14,17]
C_T	1×10^{-8}	5×10^{-7} TIF [19]	[11]
C_S	3×10^{-7}	4×10^{-7} Tl [4]	[11]
$\varepsilon_q^{\text{SUSY}}$	2×10^{-3}	1×10^{-2} n [3]	[1]
$\varepsilon^{\text{Higgs}}$	$0.4/\tan\beta$	$0.7/\tan\beta$ Tl [4]	[1]
x^{LR}	1×10^{-3}	1×10^{-2} n [3]	[1]

TABLE I. Summary of limits (95%C.L.) set by the ^{199}Hg EDM and other experiments on model-independent and “naturalness” parameters.

hadronic and semi-leptonic CP-violating effects which are summarized in Table I. The EDM of the ^{199}Hg atom is proportional to the Schiff moment of the ^{199}Hg nucleus S , which is a measure of the difference between the distributions of the electric charge and electric dipole moment in the nucleus. Using a Hartree-Fock calculation for Hg atomic wavefunctions [9] and a simple nuclear shell model [10,11] the Schiff moment has been calculated with an uncertainty of about 30-50%: $d(^{199}\text{Hg}) = -3.1 \times 10^{21} S \text{ cm}^{-2}$ [11]. The largest contribution to the Schiff moment comes from a CP-violating nucleon-nucleon interaction $\xi G_F(\bar{p}p)(\bar{n}i\gamma_5 n)/\sqrt{2}$. It was calculated in [10] using Woods-Saxon potentials and neglecting many-particle correlations. The result is $S = -1.8 \times 10^{-7} \xi e \text{ fm}^3$ with an uncertainty of about 50%. Possible enhancements of the Schiff moment due to collective octupole nuclear excitations have been considered recently in [12], although no definite estimates exist. As shown in [13,14], the CP-odd nucleon-nucleon interaction is dominated by π^0 exchange and is proportional to the pion-nucleon CP-odd coupling constant $\bar{g}_{\pi NN}$.

A limit on $\bar{g}_{\pi NN}$ can be used to directly constrain the CP-violating QCD vacuum angle $\bar{\theta}_{\text{QCD}}$ [15]. We obtain $|\bar{\theta}_{\text{QCD}}| < 1.5 \times 10^{-10}$, improving the limit set by the neutron EDM [3,16] by a factor of 4. We can also set a limit on a linear combination of chromo-EDMs of the quarks [14],

$$e|\tilde{d}_d - \tilde{d}_u - 0.012\tilde{d}_s| < 7 \times 10^{-27} e \text{ cm}.$$

This limit can be compared with a constraint on a different combination of EDMs and chromo-EDMs set by the neutron EDM experiment [3,17],

$$|e(\tilde{d}_d + 0.5\tilde{d}_u) + 1.3d_d - 0.3d_u| < 1.1 \times 10^{-25} e \text{ cm}.$$

In most extensions of the SM, including Supersymmetry, EDMs and chromo-EDMs of the quarks have comparable size [1]. We also place new constraints on semileptonic CP-violating parameters C_S and C_T , which are significant for certain multi-Higgs models [18].

In addition to the model-independent constraints discussed above, one can set limits on specific CP-violating

parameters in various extensions of the SM. For example, in the Minimal Supersymmetric SM the limit on the ^{199}Hg EDM can be used to set tight constraints on a linear combination of two CP-violating phases [14]. In Table I we only give general limits for “naturalness” parameters, as defined in [1], for Supersymmetric, multi-Higgs, and Left-Right symmetric models. For example, in Supersymmetry $\varepsilon_q^{\text{SUSY}}$ would be close to unity if the masses of supersymmetric particles were on the order of 100 GeV and CP-violating phases were large.

In conclusion, we have presented the results of a new search for a permanent electric dipole moment of ^{199}Hg atoms, improving the previous limit by a factor of 4. We have set new limits on $\bar{\theta}_{\text{QCD}}$, quark chromo-EDMs, and CP violation in various extensions of the Standard Model. We are presently upgrading the experiment and plan to improve the statistical sensitivity by at least a factor of 2. We would like to thank Warren Nagourney for help with the laser quadrupling system, Jim Jacobs for assistance in fabrication of the EDM cells, and Blayne Heckel for helpful discussions. This work was supported by NSF Grant No. PHY-9732513.

-
- [1] S. M. Barr, Int. J. Mod. Phys. A **8**, 209 (1993).
 - [2] M. Trodden, Rev. Mod. Phys. **71**, 1463 (1999).
 - [3] P.G. Harris *et al.*, Phys. Rev. Lett. **82**, 904 (1999).
 - [4] E.D. Commins, S.B. Ross, D. DeMille, and B.C. Regan, Phys. Rev. A **50**, 2960 (1994).
 - [5] J.P. Jacobs, W.M. Klipstein, S.K. Lamoreaux, B.R. Heckel, and E.N. Fortson, Phys. Rev. A **52**, 3521 (1995).
 - [6] D.M. Harber and M.V. Romalis, Phys. Rev. A (in press) (2000).
 - [7] C. Ciofi, R. Giannetti, V. Dattilo, and B. Neri, Proc. IEEE Instr. Measur. Tech. Conf., Ottawa, 1486 (1997).
 - [8] M.V. Romalis and E.N. Fortson, Phys. Rev. A **59**, 4547 (1999), S.K. Lamoreaux and E.N. Fortson, Phys. Rev. A. **46**, 7053 (1992).
 - [9] A.M. Martensson-Pendryll, Phys. Rev. Lett. **54**, 1153 (1985).
 - [10] V.V. Flambaum, I.B. Khriplovich, and O.P. Sushkov, Phys. Lett. **162B**, 213 (1985).
 - [11] I.B. Khriplovich and S.K. Lamoreaux, *CP Violation without Strangeness*, Springer, Berlin (1997).
 - [12] J. Engel, J.L. Friar, A.C. Hayes, Phys. Rev. C **61**, 035502 (2000).
 - [13] V.M. Khatsymovsky, I.B. Khriplovich, and A.S. Yelkhovsky, Ann. Phys. **186**, 1 (1988).
 - [14] T. Falk, K.A. Olive, M. Pospelov, and R. Roiban, Nucl. Phys. **B560**, 3 (1999).
 - [15] R.J. Crewther, P. Di Vecchia, G. Veneziano, and E. Witten, Phys. Lett. **88B**, 123 (1979); **91B**, 487(E) (1980).
 - [16] M. Pospelov and A. Ritz, Phys. Rev. Lett. **83**, 2526 (1999).
 - [17] M. Pospelov and A. Ritz, hep-ph/0010037.
 - [18] S. M. Barr, Phys. Rev. Lett. **68**, 1822 (1992).
 - [19] D. Cho, K. Sangster, and E. A. Hinds, Phys. Rev. Lett. **63**, 2559 (1989).